BNL--46550

DE92 000127

NUMERICAL SIMULATIONS OF TURBULENT FLOW FIELDS CAUSED BY SPRAYING OF WATER ON LARGE RELEASES OF HYDROGEN FLUORIDE

V. M. Fthenakis and K. W. Schatz

May 1991

Prepared for presentation at the ASME 1991 Symposium
on Fluid Mechanics of Sprays
Atlanta, GA, December 4-6, 1991

BIOMEDICAL AND ENVIRONMENTAL ASSESSMENT DIVISION
DEPARTMENT OF APPLIED SCIENCE
BROOKHAVEN NATIONAL LABORATORY
ASSOCIATED UNIVERSITIES, INC.

Under Contract No. DE-AC02-76CH00016 with the
U. S. Department of Energy

NUMERICAL SIMULATIONS OF TURBULENT FLOW FIELDS CAUSED BY SPRAYING OF WATER ON LARGE RELEASES OF HYDROGEN FLUORIDE

V.M. Fthenakis
Brookhaven National Laboratory, Department of Applied Science, Upton, NY 11973.

K.W. Schatz
Mobil Research and Development Corp., PO Box 1026, Princeton, NJ 08540.

ABSTRACT

The effectiveness of water sprays in absorbing HF releases was recently demonstrated in extended laboratory and field tests. In this paper, computer simulations are presented of the Hawk, Nevada Test Site, series of field tests. The model used, HFSPRAY, is a Eulerean / Lagrangian model which simulates the momentum, mass and energy interactions between a water spray and a turbulent plume of HF in air; the model can predict the flow velocities, temperature, water vapor, and HF concentration fields in two-dimensional large-geometries for spraying in any direction, (i.e., down-flow, inclined-down-flow, up-flow, and co-current horizontal flow). The model was validated against recent data on spraying of water on large releases of HF.

1. INTRODUCTION

Releases of hydrofluoric acid (HF) can be effectively controlled in the field by absorption using water sprays (Blewitt et al, 1987; Schatz & Koopman, 1989). The feasibility of this control option also was studied theoretically (Fthenakis, 1989; Fthenakis & Zakkay, 1990). In this paper, we discuss the results of modeling the Hawk field tests, which were conducted at the DOE Nevada Test Site in 1988, under the auspices of the Industry Cooperative HF Mitigation/Assessment Program (Schatz & Koopman, 1989). The model used in these simulations, HFSPRAY, is based on the PSI-Cell Computer code (Crowe et al., 1977).

2. DESCRIPTION OF MODEL

The HFSPRAY model comprises two sets of equations, one describing the gas-phase, and the other describing the drop-phase. The gas-phase is modeled, by an Eulerean approach, as a continuous fluid at steady state with properties changing with distance, in two-dimensional coordinates. The liquid-phase is modeled according to a Lagrangian approach by considering a finite number of particles of varying size and trajectory (Crowe et al 1977).

2.1 Gas-Phase Equations

Conservation of Mass

$$\frac{\partial}{\partial x}(\rho u) + \frac{\partial}{\partial y}(\rho v) = M$$

where M is the change in the mass of the drops per unit volume and unit time.

Conservation of Momentum

x-component

$$u\frac{\partial}{\partial x}(\rho u) + v\frac{\partial}{\partial y}(\rho u) = -\frac{\partial P}{\partial x} + 2\frac{\partial}{\partial x}\left(\mu_e\frac{\partial u}{\partial x}\right) + \frac{\partial}{\partial y}\left(\mu_e\left(\frac{\partial u}{\partial y} + \frac{\partial v}{\partial x}\right)\right) - \frac{2}{3}\frac{\partial}{\partial x}\mu_e\left(\frac{\partial u}{\partial x} + \frac{\partial v}{\partial y}\right) + F_x$$

y-component

$$u\frac{\partial}{\partial x}(\rho v) + v\frac{\partial}{\partial y}(\rho v) = -\frac{\partial P}{\partial y} + 2\frac{\partial}{\partial y}\left(\mu_e\frac{\partial v}{\partial y}\right) + \frac{\partial}{\partial x}\left(\mu_e\left(\frac{\partial u}{\partial y} + \frac{\partial v}{\partial x}\right)\right) - \frac{2}{3}\frac{\partial}{\partial y}\left(\mu_e\left(\frac{\partial u}{\partial x} + \frac{\partial v}{\partial y}\right)\right) + \rho g + F_y$$

The 2/3 ∇u terms are included in the Navier-Stokes equations to describe the mixing of HF with air. F_x and F_y are the components of the total force from the drops, per unit volume. The spatial distribution of these force components is obtained from the solution of the drop-phase equations.

k-ε turbulence model

$$\frac{\partial}{\partial x}(\rho u k) + \frac{\partial}{\partial y}(\rho v k) = \frac{\partial}{\partial x}\left(\frac{\mu_e}{\sigma_k}\frac{\partial k}{\partial x}\right) + \frac{\partial}{\partial y}\left(\frac{\mu_e}{\sigma_k}\frac{\partial k}{\partial y}\right) + G$$

$$- C_o \rho \epsilon$$

$$\frac{\partial}{\partial x}(\rho u \epsilon) + \frac{\partial}{\partial y}(\rho v \epsilon) = \frac{\partial}{\partial x}\left(\frac{\mu_e}{\sigma_\epsilon}\frac{\partial \epsilon}{\partial x}\right) + \frac{\partial}{\partial y}\left(\frac{\mu_e}{\sigma_\epsilon}\frac{\partial \epsilon}{\partial y}\right) + \frac{C_1 \epsilon G}{k} - \frac{C_2 \rho \epsilon^2}{k}$$

From k and ϵ, the effective viscosity is determined from the Prandtl-Kolmogorov formula.

$$\mu_e = C_\mu \frac{\rho k^2}{\epsilon}$$

$$G = 2\mu_e \left[\left(\frac{\partial u}{\partial x}\right)^2 + \left(\frac{\partial v}{\partial y}\right)^2\right] + \mu_e \left(\frac{\partial u}{\partial y} + \frac{\partial v}{\partial x}\right)^2$$

G is the rate of generation of k due to Reynolds stresses, $\rho\epsilon$ is the rate of dissipation of k, and σ_κ, σ_ϵ, C_1, C_2, & C_μ are empirical constants.

Conservation of Species

$$\frac{\partial}{\partial x}(\rho u Y_i) + \frac{\partial}{\partial y}(\rho v Y_i) = \frac{\partial}{\partial x}\left(\rho D_e \frac{\partial Y_i}{\partial x}\right) + \frac{\partial}{\partial y}\left(\rho D_e \frac{\partial Y_i}{\partial y}\right) - W$$

where Y_i is the molar fraction of HF and of water vapor, D_e the corresponding diffusivity, and W the sink term representing absorption or evaporation per unit volume. The sum of W terms in the species equations is equal to the source term, M, of the continuity equation.

Conservation of Energy

$$\frac{\partial}{\partial x}(\rho u T) + \frac{\partial}{\partial y}(\rho v T) = \frac{\partial}{\partial x}\left(\frac{k}{c_{pg}}\frac{\partial T}{\partial x}\right) + \frac{\partial}{\partial y}\left(\frac{k}{c_{pg}}\frac{\partial T}{\partial y}\right) + Q$$

where k is thermal conductivity, c_{pg} is the specific heat of the air mixture and Q the term representing rate of heat exchange with drops in a unit volume.

Equation of State

Substitution of expressions for mixture molecular weight in the ideal gas law results in:

$$\frac{\rho}{\rho_o} = \frac{T}{T_o} \frac{18\ MW_{HF}}{(18+11\ y_w)(MWHF + (29 - MW_{HF})\ y_{HF}}$$

The above equations are solved with wall, no-slip conditions on the floor, and either wall or free-stream conditions at the top boundary.

2.2 Droplet-Phase Equations

Momentum Transfer

The single drop trajectory equations are described by Crowe et al. (1977); for our application, we changed the drag coefficients. For Re numbers greater than 400, Buzzard's and Nedderman's (1987) experimental data are used; for lower Re the following equations proposed by Beard and Pruppacher (1971) are used:

$$C_D = (24/Re)(1+0.11\ Re^{0.81}) \qquad Re<21$$
$$C_D = (24/Re)(1+0.189\ Re^{0.632}) \qquad 21<Re<400$$

These coefficients were adjusted for drop multiplicity, as described below.

Mass transfer

The mass sink terms in the gas-phase equations are determined from calculations based on an individual drop. The molar flux of a gas A passing through the surface of a drop is denoted by N_A where

$$N_A = K_g(Y-Y^*)$$

and the amount of gas A absorbed by a drop of diameter d during its time of passage (Δt) through the reference volume is

$$W = \pi d^2 \int_0^{\Delta t} K_g(Y-Y^*)dt$$

where the superscript * indicates phase equilibrium conditions.

The term W is the total absorption by all drops in the reference volume and is estimated from the double sum over trajectory segments and drops in each segment.

$$W = \sum_i^{nt} \sum_j^{np} w_{i,j}$$

K_g is the overall mass transfer coefficient based on the gas-phase, which is related to the individual gas and liquid mass-transfer coefficients, k_g and k_l, by:

$$1/K_g = 1/k_g + H^*/k_l$$

where H^* is a pseudo-Henry's law coefficient accounting for the totality of disolved species (Fthenakis, 1989); k_g is estimated from the Ranz-Marshall relationship for the Sherwood number, and k_l from Angelo et al's model (1966).

The build-up of average concentration of the dissolved fluorides into the drop is determined from

$$C_A \Big|_0^{\Delta t} = \frac{w}{V} \Delta t$$

where V = drop volume= $\pi d^3/6$

Energy Transfer

The energy equation for a single drop can be written as:

$$m\ C_p \frac{dT}{dt} = Nu\ \kappa\ \pi\ d\ (T_g - T_p) - \dot{m}_w\ h_g - \dot{m}_{HF}\ h_{HF}$$

where m is the drop mass, $\dot{m}_w$ the drop evaporation rate,
$\dot{m}_{HF}$ the drop absorption rate of HF
h_g latent heat for water evaporation
h_{HF} heat of solution for HF(g)+H_2O mixing

In the solution of this equation, we use Clasius-Clayperon equation for the dependance of water vapor pressure on temperature, and Shotte's (1988) equations for the dependance of water vapor pressure on the HF composition in the drop.

$$P_w = e^{A+(B/T)}$$

where $A = 14.2941 - 0.820699\ Y_{HF} - 2.91643\ Y_{HF}^2$
$B = -5297.8 - 76.4864\ Y_{HF} + 108.11\ Y_{HF}^2$
P_w is the partial vapor pressure in the drop,
Y_{HF} is the molar fraction of HF in the drop, and T the absolute temperature (^oK).

2.3 Multiple Drop Analysis

Analysis at a micro-scale level (i.e., one drop) gave us relationships that can be used in the aggregated macro-level system. However, single-drop relationships, cannot be used *a priori*. These relationships assume that the drops do not perturb the flow velocity field, which is a reasonable assumption for studies of gas scavenging by rain, but not for spray systems.

Two separate regions of flow are considered, where drop-gas-drop interactions can change the momentum, mass, and energy transfer coefficients predicted by single-drop relationships. These regions are i) near the nozzle at high flow rates of water, (dense spray) when the drops occupy a significant fraction (e.g. >0.05) of the volume of the gas-phase, and ii) farther away from the nozzle where drop trajectories are separated and we need only to consider the effect of drops following each other in a line. In the first region the following relationships (O'Rourke, 1981), are used to adjust the momentum, coefficients:

$$\frac{C_D}{C_{DS}} = 1 + 3.5\,\phi$$

$$Sh = 2\,(1-\phi)^{-1.75} + 0.6\,\left(\frac{Re}{(1-\phi)}\right)^{1/2} Sc^{1/3}$$

$$Nu = 2\,(1-\phi)^{-1.75} + 0.6\,\left(\frac{Re}{(1-\phi)}\right)^{1/2} Pr^{1/3}$$

These adjustments have been found to be significant for high flow rates of water in regions near the nozzle.

In the rest of the region the population of drops is small and the drops follow each other on trajectories. Then the motion of the gas induced by the preceding drops can reduce the resistance to the movement of the following drops. Ramachandran (1985) proposed relationships correlating a decline in C_D with the size of the drop and with drop-to-drop distance. According to his relationships a maximum decline of 30 % can occur for drops of 300 μm diameter. In our simulations, we adopt a 15 % reduction in the drag coefficient due to this effect.

<u>The Effect of High Mass-Transfer on Momentum, Mass and Heat Transfer Coefficients</u>

HF absorption in drops can be so fast that it alters the velocity, concentration, and temperature profiles through the drop interface. To describe these phenomena, we determined the correction factors for the drag, mass, and heat transfer coefficients, following the film theory outlined in Bird et al., 1960; (pp. 656-668).

Mass transfer from the gas-phase into the drop makes the correction factors greater than unity and results in higher transfer coefficients, whereas the reverse direction of flow through the interface reduces the transfer coefficients. Therefore, the mass transfer coefficient for absorption will increase, whereas the evaporation and the heat transfer coefficients will decrease. For the simulations of HF releases presented below, the combined effects of absorption and evaporation on the drag coefficient counter-balanced each other, whereas the correction factors on the mass and heat-transfer coefficients ranged from 0.95 to 1.05.

3. MODEL VALIDATION WITH THE DATA FROM HAWK FIELD TESTS

An *ad hoc* Industry Cooperative HF Mitigation / Assessment Program, sponsored and funded by 20 U.S. companies produced, in June 1989, a series of laboratory and field data on the mitigation of HF releases by water sprays. The field series, called the Hawk HF Test series, included 87 tests carried out in a flow chamber at the Nevada Test Site outside Mercury, Nevada. The chamber was 8 ft wide, 16 ft high, and 140 ft long and had a wind screen, inlet funnel, flow straightener and turbulence grid to achieve even flow and turbulence. Tests were done by releasing the acid horizontally, typically at a rate of 2 to 5 gpm for 10 minutes, through an orifice in the front section of the chamber. A water curtain with 8 nozzles sprayed water perpendicularly on the acid jet. In other tests, the interaction was counter-current with a single monitor downwind of the HF release. The efficiency of removal of HF was calculated from concentration and volume measurements of the collected acidic water, and from air samples.

The model estimates were compared with data from the 87 field test data covering down-flow, upflow and counter-current horizontal flows, and variations of the following parameters: 1) Water flow, 2) Drop size, 3) Distance of spray header, 4) Elevation of spray , 5) Wind speed, 6) Humidity, 7) Pressure in HF storage, and 8) Angle of monitor. The model predictions agree within +-6 % with most of the field data and they also match the visual observations in the field (Schatz and Koopman, Vol I, 1989, pp. 155-163).

The Hawk field tests were simulated by a two-dimensional configuration, in a plane that represents the downwind (x), and height (y) dimensions. The grids of the numerical solution were sufficiently fine to result in i) solutions which are insensitive to further reductions of the grid size, and ii) small mass errors (typically <3% based on the continuity). To simulate monitor flow, a 20x40 grid was sufficient for most practical applications, whereas in down-flow simulations at high rates of water flow, the strong turbulence induced close to the floor necessitated much finer grids (e.g., 40x60 to 60x90). Convergence was easier to obtain by iterating for the velocity fields and energy fields decoupled from mass transfer, before going into the complete iteration cycle.

<u>3.1 Inlet Boundary Conditions</u>

In the simulations described herein, the heavy gas atmospheric dispersion model HFPLUME (Puttock et al, 1990) was used to estimate the thickness and velocity of an HF jet released from a pressurized container; these values were used as inlet boundary conditions to HFSPRAY. Plume velocities between 3.6 and 7 m/s and wind velocities of 3 m/s and 6 m/s were used.

The HF plume is assumed to initially spread across the whole width of the chamber, while maintaining its thickness and relative position in respect to the floor and the nozzles. In other words, the circular plume is represented two-dimensionally by a rectangular slab of height equal to the diameter of the plume and width equal to the chamber width; then the inlet HF concentration is internally calculated to match the field HF mass flow rate.

3.2 Air Entrainment

The rate of air entrainment into an 8-nozzle water curtain was estimated in the laboratory by measuring the velocity of air flowing out of the curtain at floor level. Velocity profiles for two sets of nozzles, at elevations of 3.25 m and 5.7 m from the floor, are given in Table E5-1 of volume III of Schatz & Koopman (1989). Comparisons of these data with values of velocities predicted by the model, are reported by Fthenakis (1991); a sample comparison is shown in Figure 1. The estimated velocity profiles fit within the range of the experimental data, although they do not decrease with height as much as the actual data.

Fig. 1 Air Entrainment Velocities TF16FCN Nozzles at 5.7 m Elevation

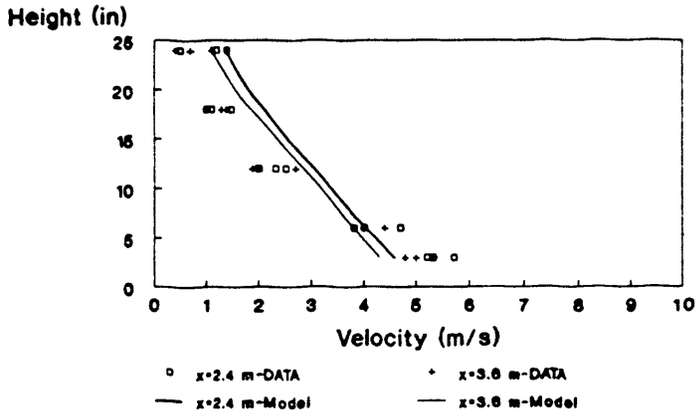

These modeling exercises of air entrainment, directed us towards a refinement of the parameters of the k-ε turbulence (Launder and Spalding, 1972). Through numerical experimentation, the value of the empirical parameter (C_1), for the generation of the turbulence kinetic energy was changed to 1.07, from 1.45 used in the standard k-ε model. The value of the dissipation constant (C_D), was also changed since it is correlated to C_1 by $C_D = k^2/(C_2-C_1)C_\mu^2$
Also the floor boundary conditions were changed to include the roughness of its surface.

3.3 Estimates of Water Collection

The predicted distances and heights that drops travel within the chamber match the visual observations in the field. Also, the estimated quantities of water that drop out on to the floor compare very well with the field data on water collection; a sample of these comparisons is shown in Figure 2.

Fig. 2 TF20FCN-UPFLOW Spray Distribution from Water Collection

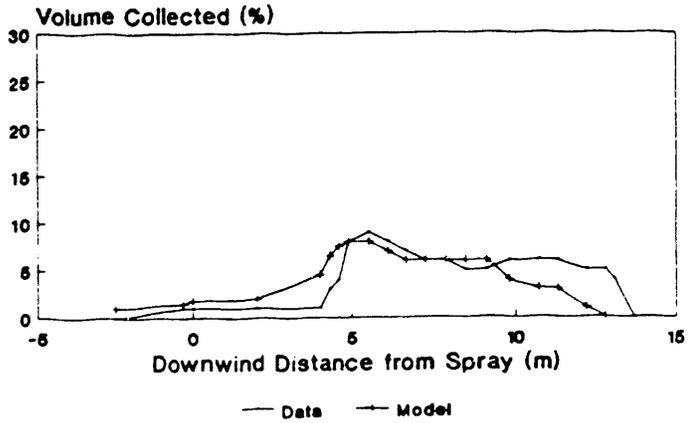

3.4 HF Saturation in Water Drops

A literature survey of experimental data revealed that in humid air the maximum concentration of HF within drops is much lower than the theoretical maximum (Gmelin, 1982; Zaytsev et al, 1970; Butvin et al, 1979). These data show that at concentrations of water vapor higher than 1.5 times the HF concentration, the absorption of HF is significantly reduced, and can cease completely within one second, although the concentration built-up in the drop is only a very small fraction of the saturation maximum of 62.5 wt %. This behavior is described in the model by an exponential decay of the mass transfer coefficient, starting after 1 s of interaction at high water concentrations. This adjustment resulted to significantly lower estimates for the lowest water to HF ratios (e.g. Ratio < 13) than the estimates generated assuming a 62.5 % maximum saturation concentration.

3.5 Base Case: Down-Flow

The base case simulations refer to down-pointing sprays with a varying water/HF mass ratio; the HF flow rate was essentially constant here, while the water flow rate varied. Figure 3 shows the model estimates and the corresponding experimental data; the estimates fit the data within 6 %.

Fig. 3 Down-Flow: Comparison of Model Estimates with Hawk Field Data

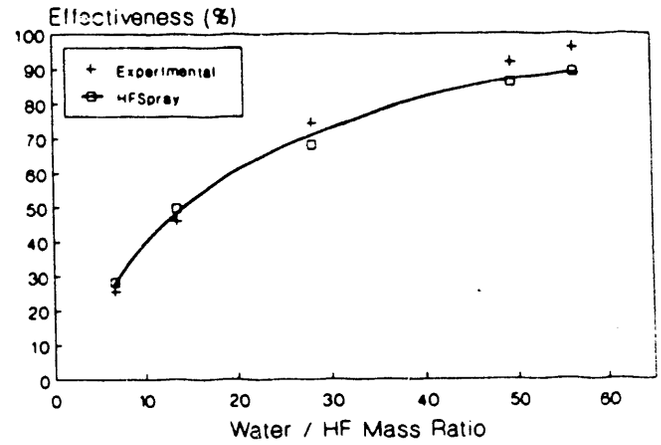

Figures 4-6 display the predicted velocity vectors, the HF concentration contours, and the spray outer trajectories. The initial air velocity is about 3 m/s, and the velocity of the HF plume varies from 3.6 to 5 m/s, depending on the HF flow rate. The zones between specific concentration contours (wt %) are displayed in different shades. The plume enters at a uniform initial concentration of about 4 wt %; the plots show its dilution down to 0.01 wt % (100 ppm). In all the simulations of the base case, the flow rates of the HF plume are approximately constant, while the water flow rates increase from Figure 4 to Figure 6. The outer trajectories of all drop sizes are shown by dotted lines originating at Height=2.45 m and Downwind Distance=4 m.

Figure 4 (Test 1) shows spraying at the lowest water flow used in the field (1.57 kg/s); in this simulation, very little lift is predicted at the spray region and a long plume is formed downwind of the spray. In the intermediate and high water flows (Figures 5 & 6), the HF plume encounters a recirculation zone just upstream of the spray, which enhances HF-air mixing. As the water flow increases, this recirculation becomes more intense and covers a

Fig. 4 TEST1-DOWNFLOW Hawk Field Tests -Eff=27.3 %-

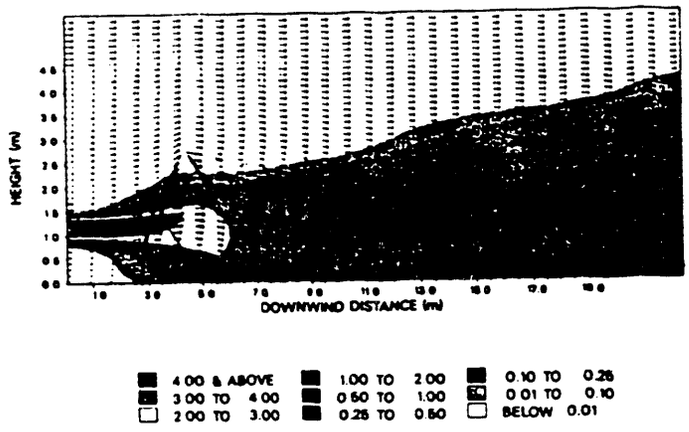

Fig. 5 TEST4-DOWNFLOW Hawk Field Tests -Eff=74.8 %-

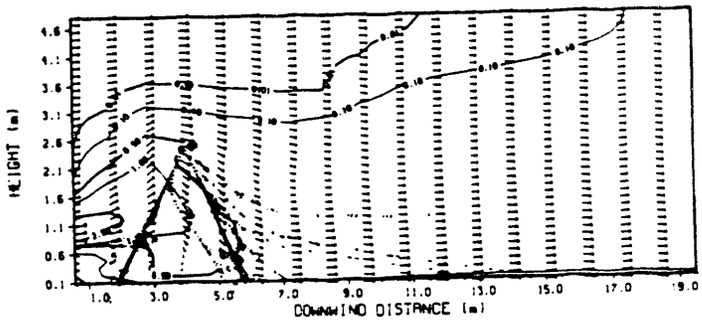

Fig. 6 TEST5-DOWNFLOW Hawk Field Test -Eff=89.3%-

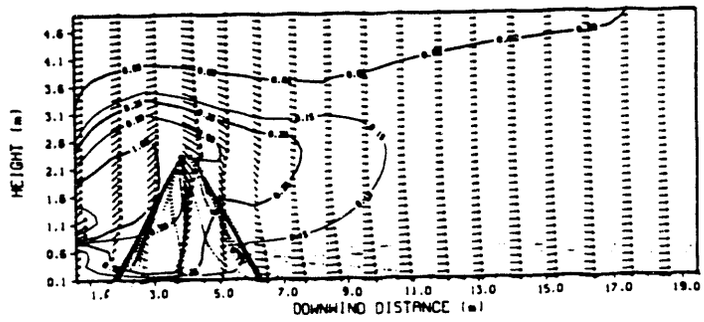

larger region. In Test 4, (shown in Figure 5) a higher water flow-rate (6.35 kg/s) lifts the plume upwind of the spray; a recirculation zone is induced within the spray region, which brings the plume down again and effectively mixes it with water. The higher the water flow, the more the HF plume is deflected upwards at the upwind side of the spray, and subsequently pulled down at the downwind side of the spray as more air is drawn in the spray. At the highest flow rates (12.5 kg/s; Fig. 6), increased recirculation induces a stronger floor jet and turbulence. The plume is lifted higher before it is trapped in the recirculation zone for effective scrubbing.

The fit of the model estimates at low and intermediate water flows (i.e., ratios) is better than the fit of the high ratio estimates (Figure 3). For Ratio=64 the model predicts a 90 % HF removal versus 96 % measured in the field. According to field observations, in this test a dynamic effect was happening above the spray nozzle, with the plume periodically being lifted to the ceiling and then collapsing down in to the spray region. This effect cannot be described by a steady-state model, such as HFSPRAY.

3.6 Wind Speed

As shown in Fig. 7, the model predicts a significant decline in the effectiveness of HF absorption with increasing wind speeds from 3 m/s to 10 m/s, whereas increases from 1.2 m/s to 3 m/s had a negligible effect. This decline of effectiveness with increasing wind speed is much more profound in low water-flow rates than in high ones. This effect happens because, at high water flows, the spray carries sufficient momentum to deflect and stop the HF plume, whereas in low flows the HF plume penetrates through the spray region. Increase in wind velocity reduces upstream recirculation, and also reduces the lateral spreading of the HF plume; both these factors reduce the effectiveness of mass transfer.

Fig. 7 Effect of Wind Speed Variations
(Downflow, Hawk Field Configurations)

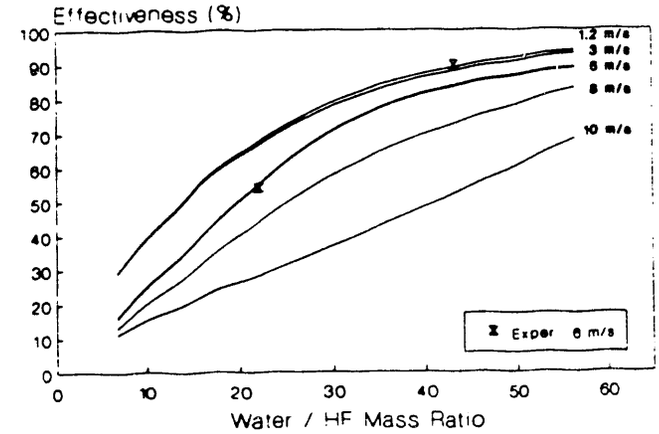

3.7 Up-Flow

The model estimates that more HF will be removed in upflow-spraying than in downflow at the same ratios and configurations (e.g., nozzle elevation, plume elevation) as in the field. The predicted trajectories, velocities, and concentration fields match very well with the visual field observations. The model fits well the low- and high-ratio data, but it underestimates by about 13 % the single data point

Fig. 8 Model Simulations of HF Field Data
Upflow vs DownFlow

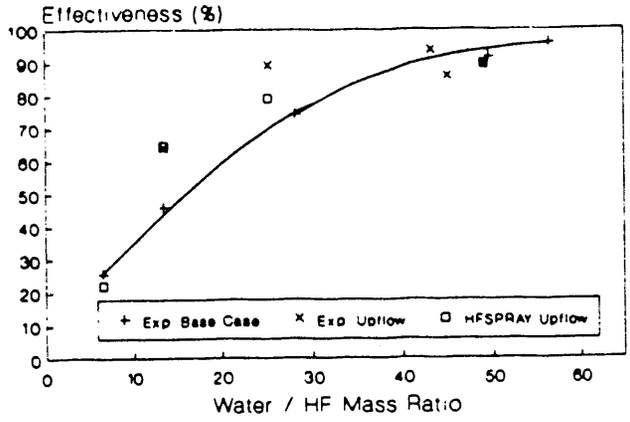

Fig. 9 TEST22-UPFLOW Hawk Field Test -Eff=84.7 %-

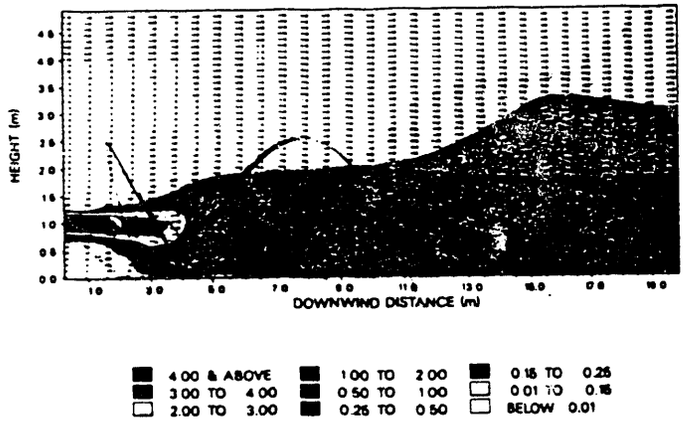

Fig. 10 TEST23-UPFLOW Hawk Field Test -Eff=89.6 %-

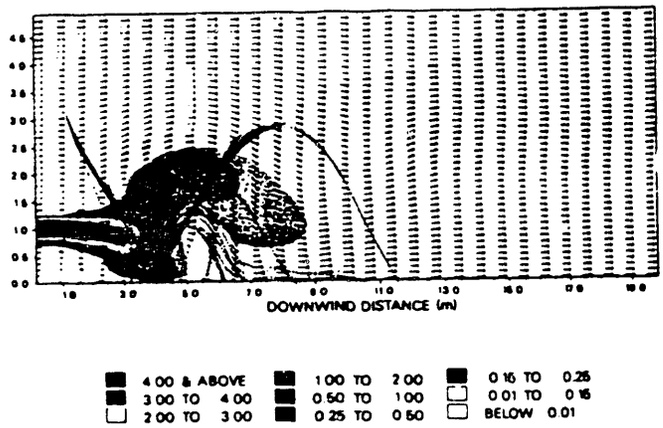

at the intermediate ratio (Figure 8). Figures 9-10 show the predicted velocity vectors, outer drop trajectories and concentration contours for different water flows (ratios 12.4 & 48.9, correspondingly). The spray nozzle is at 0.1 m off the floor. The outer trajectories of drops of 55, 110, 225, 450, and 700 microns are shown in these plots. At ratio=12.4 the biggest drops reach a height of 2.5 m, penetrating through the plume, whereas the smaller ones start falling earlier. The HF plume flows horizontally and is lifted further downwind by thermal buoyancy and mixing.

In Test 23, (see Fig. 10) the highest water flows (12.5 kg/s) were used and more drops with a higher momentum are produced. The drops reach a height of about 3.2 m, and induce a recirculation zone near the spray's nozzle. The HF plume hits the spray and is reflected slightly downward, inducing a lot of mixing in the spray region, with strong turbulence at the bottom of the plume; then, the HF plume flows higher, filling the chamber to the ceiling.

These results confirm that upflow is more effective (about 13% more) than downflow at the same flow rates and plume elevation. However, more parametric studies are required to determine the limits of the effectiveness of upflow. The effectiveness of upflow spraying is expected to be reduced with increasing nozzle-to-plume distance, to a greater extent than in downflow, since in upflow the drops may not penetrate through the plume.

3.8 Counter-Current Flow

In these simulations, a narrow monitor sprays from 15 m downwind and is directed towards the point of release at 20° from the horizontal. An initial spray angle of 3°, and drop diameters of 1.2, 0.8, and 0.5 mm (mean size = 1 mm) were assumed. The drops travel up to a height of 3.8 m and then fall down on the plume close to the point of release; their spread at the top of the cloud is about 1 m. The 1 mm drops are not carried downwind, and practically all the absorption occurs in a narrow zone within 1 m from the point of release (Fig. 11).

Fig. 11 NARROW MONITOR Hawk Field Test #26 (R-58) -Eff=74 %-

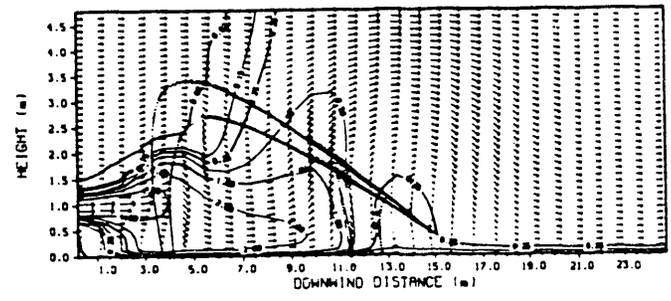

4. SENSITIVITY STUDIES

Simulations using a 20x40 grid size and 12 trajectories with five drop sizes were very fast (a few

minutes of CPU time on a VAX3650). A 20x40 grid can qualitatively describe most of the effects we have discussed, but a finer grid is needed for accurate estimates. Table I shows effectiveness obtained from grids of different size: for upflow (and, similarly, for downflow) a 40x60 grid is required, although for counter-current flows (monitor), a 20x40 grid can be sufficient for practical applications. For the coarse (20x40) grid, 10 trajectories are sufficient but the finer grid requires up to 30 trajectories (see Table II). Using only two trajectories resulted to gross deviations.

Table I. Effectiveness (%): Sensitivity to Grid Size

Grid Size:	20x20	20x40	40x40	40x80	40x90	50x90
Test#10:	46.5	54.	71.4	74.4	74.8	76.2
Test #24:	42.8		46.1			

Table II. Effectiveness (%): Number of Trajectories

Grid Size:	20x20			40x60	
Trajectories # :	2	10	30	30	60
Upflow Test#10:	56.	45.3	46.5	74.4	75.2
Monitor Test #24:	18.	43.5	42.8	48.8	46.4

Using a uniform concentration profile for HF in the inlet, instead of an equivalent, parabolic concentration profile, gave about 3% difference in absorption effectiveness for sample runs (Table III). The effects of using rough approximations for drop size was also found to be sizable (Table III).

Table III. Uniform vs Parabolic Inlet Concentration Profile

Test #	Ratio	Uniform Effectiveness (%)	Parabolic Effectiveness (%)
Test 4	28.1	65.2	67.4
Test 17	49	81.2	84.

Table IV. Drop Size Distribution vs Mean Drop Size

Test #	Ratio	Distribution Effectiveness (%)	Mean Effectiveness (%)
Test 4	28.1	67.4.	69.2
Test 17	49	84.2	82.2.

CONCLUSIONS

Large-scale field experiments have demonstrated that absorption of a gas by water spraying can be a very effective mitigation option of unconfined releases of highly water-soluble hazardous gases.

The model HFSPRAY describes the momentum, mass, and energy interchange between the water drops and the surrounding gas-phase, as well as of chemical reactions in the drop phase. This model was validated against all the field data involving HF releases. The estimates of HF removal fit very well with these experimental data, and the predicted turbulence flow fields match the air entrainment data and the visual observations in the field.

The spray's effectiveness increases with increasing water flow, and decreasing drop size, as shown by both the field data and the model estimates. Other influencial parameters include the distances from nozzle-to-plume, and nozzle-to-ground distances which are pivotal in deciding if upflow is better than downflow, or vice versa. Several more parameters influence the effectiveness of absortion effectiveness, and the model provides the tool to study specific applications.

ACKNOWLEDGEMENTS

The authors are thankful to Prof. C.T. Crowe for providing the PSI-Cell program. Many thanks also are due to Drs. V. Zakkay, U.S. Rohatgi, S. Morris, P.D. Moskowitz, and A. Bulawka for helpful discussions.
This research was supported, in part, from the Industry Cooperative HF Mitigation / Assessment Program, and the Photovoltaic Energy Technology Division, Conservation and Renewable Energy, U.S. Department of Energy.

REFERENCES

Angelo J.B., Lightfoot E.N., and Howard D.W., Generalization of the penetration theory for surface stretch: Application to forming and oscillating drops, AIChE Journal, 12(4), 751-760, (1966).

Beard, K.V., and Pruppacher H.R., A wind tunnel investigation of the rate of evaporation of water drops falling at terminal velocity in air, J.Atmos.Sc. 28, 1455-1464, (1971).

Bird R. B., Stewart W.E. and Lightfoot E.N., Transport Phenomena, Wiley, NY, 1960.

Blewitt, D.N.,Yohn J.F., Koopman R.P., Brown T.C., and Hague W.J., Effectiveness of water sprays on mitigating anhydrous hydrofluoric acid releases, Proceedings of the International Conference on Vapor Cloud Modeling, pp. 155-171, Nov 2-4, 1987, published by the American Institute of Chemical Engineers, (ed. J. Woodward).

Butvin, A.N. et. al, Absorption of Hydrogen Fluoride by Drops of Liquid, Chem. Abst., Vol. 91, No 28125, 1979, p.488.

Buzzard J.L., and Nedderman R.M., Chem. Eng. Sci., 22, 1577, (1967).

Crowe C.T., Sharma M.P. and Stock D.E., The Particle-Source-In Cell (PSI-CELL) model for Gas-Droplet Flows, J. Fluids Eng., 99(2), 325-332, (1977).

Fthenakis, V.M. and Zakkay V., A Theoretical Study of Absorption of Toxic Gases by Spraying, *Journal of Loss Prevention*, 3, 197-206, 1990.

Fthenakis, V.M., The feasibility of controlling unconfined releases of toxic gases by liquid spraying, *Chemical Engineering Communications*, 83, 173-189 (1989).

Fthenakis, V.M., Modeling of Water Spraying of Toxic Gas Releases, Ph.D. Thesis, Department of Applied Science, New York University, 1991.

Gmelin Handbook of Inorganic Chemistry, Fluorine-Supplement Vol. 3, pp.246-247, Springer-Verlag, Berlin, 1982.

O'Rourke, P.J., Collective Drop Effects on Vaporizing Liquid Sprays, Ph.D. Thesis, Princeton, 1981.

Puttock J.S et. al, Development and Validation of Atmospheric Dispersion Models for Hydrogen Fluoride, Shell Research Limited, Chester, England, Technical Report, 1990.

Ramachandran, S., Mathematical modeling and computer simulation of mass transfer in simple multiple drop systems, Ph.D. Thesis, Rensselaer Polytech. Inst., Troy, NY (1985)

Schatz K.W. and Koopman R.P., Effectiveness of Water Spray Mitigation Systems for Accidental Releases of Hydrogen Fluoride; Industry Cooperative HF Mitigation / Assessment Program, final draft, vol I, June 1989.

Shotte, W., Collection of phase equilibrium data for separation technology, Ind. Eng. Chem. Process DEs. Dev., Vol. 19, pp. 432-439 (1980)

Zaytsev V.A. et. al, Some Peculiarities of HF and SiF_4 Absorption, The Soviet Chemical Industry, no. 9, pp. 46-48, September 1970.

END

DATE FILMED

11/14/91